

Seismic strengthening of nonductile bridge piers using low-cost glass fiber polymers

K. RODSIN¹, Q. HUSSAIN^{2*}, P. JOYKLAD^{3*}, A. NAWAZ⁴, and H. FAZLIANI⁵

¹Center of Excellence in Structural Dynamics and Urban Management, Department of Civil and Environmental Engineering Technology, King Mongkut's University of Technology North Bangkok, Bangkok, Thailand

²Center of Excellence in Earthquake Engineering and Vibration, Department of Civil Engineering, Chulalongkorn University, Thailand

³Department of Civil and Environmental Engineering, Faculty of Engineering, Srinakharinwirot University, Thailand

⁴Department of Civil Engineering, COMSATS University, Wah Campus, Wah Cantt., Pakistan

⁵School of Environment, Resources and Development, Asian Institute of Technology, Thailand

Abstract. Several recent earthquakes have indicated that the design and construction of bridges based on former seismic design provisions are susceptible to fatal collapse triggered by the failure of reinforced concrete columns. This paper incorporates an experimental investigation into the seismic response of nonductile bridge piers strengthened with low-cost glass fiber reinforced polymers (LC-GFRP). Three full-scale bridge piers were tested under lateral cyclic loading. A control bridge pier was tested in the as-built condition and the other two bridge piers were experimentally tested after strengthening them with LC-GFRP jacketing. The LC-GFRP strengthening was performed using two different configurations. The control bridge pier showed poor seismic response with the progress of significant cracks at very low drift levels. Test results indicated the efficiency of the tested strengthening configurations to improve the performance of the strengthened bridge piers including crack pattern, yield, and ultimate cyclic load capacities, ductility ratio, dissipated energy capacity, initial stiffness degradation, and fracture mode.

Key words: composite materials, ductility, glass fiber, polymers, earthquake, strengthening, FRP.

1. Introduction

Several recent earthquakes in California, Japan, Central and South America have indicated that the design and construction of bridges based on former seismic design provisions are susceptible to fatal collapse triggered by the failure of reinforced concrete columns [1–3]. A significant fraction of concrete structures are in an uncertain condition [4, 5] such as columns in several existing bridges, which usually have potential problems like inadequate ductility due to inappropriate transverse confinement, improper details and deficient strength of the column/footing and column/superstructure [6–8].

A current inspection of existing reinforced concrete buildings and bridges in Thailand also revealed that most columns are designed against gravity loads only and seismic design provisions are not generally regulated [9, 10]. Significant deficiencies found in the details of typical bridges include the practice of using widely spaced stirrups and the provision of lap splices in the potential plastic hinge area [11]. Such columns and bridge piers are referred to as nonductile in the literature [9, 11, 12]. Therefore, there is a pressing requirement to improve the existing older buildings and bridges and upgrade them to recent seismic design standards. Several approaches have been proposed by various researchers for the purpose of retrofitting and repairing the concrete [13]. Generally, traditional methods of

upgrading the load-carrying capacity and ductility of structures are concrete jacketing [14, 15] and steel jacketing [16–18]. Concrete jacketing is the application of a concrete shell surrounding a member that is reinforced to enhance the strength and ductility of the element [19, 20]. However, the use of concrete jacketing involves some disadvantages such as an increase in volume and weight, artful detailing, and laborious work to install it on-site. In contrast to concrete jacketing, the steel jacketing method does not significantly increase the weight and saves construction time [18]. Nagaprasad *et al.* [21] used a steel cage to confine the concrete columns of buildings. The results showed excellent behavior in terms of flexural strength and ductility due to the external confinement from steel cages. Steel jacketing has also proved to be an efficient measure to retrofit bridge columns to increase the lateral strength and ductility [17–19] and this method has been extensively put into practice in California and elsewhere. Despite the successful application of steel jacketing in seismic strengthening, this technique involves some disadvantages such as high weight of steel plates causing difficulties during the installation and corrosion problems during the service life. There is a definite need to look for alternative ways to upgrade the retrofitting practice for the vast number of existing deficient bridge structures all over the world.

Composites are usually used as retrofitting materials primarily due to their very high strength to the mass ratio [22]. Externally bonded unidirectional fiber-reinforced polymer (FRP) systems are composites that have been in use around the world since the mid-1980s to reinforce and retrofit concrete structures [23]. FRP is a composite material consisting of two different independent elements. The key structural element is

*e-mail: ebbadat@hotmail.com, panuwatj@g.swu.ac.th

Manuscript submitted 2020-05-15, revised 2020-06-29, initially accepted for publication 2020-08-10, published in December 2020

the fibers that are encapsulated by a matrix consisting of some type of polymer [23–25]. These FRP systems were established as substitutes for conventional external reinforcing techniques such as steel plate bonding and steel or concrete column jacketing. These unidirectional FRP(s) include carbon FRP [26], glass FRP [27, 28], aramid FRP [29], polyethylene terephthalate (PET) FRP and polyethylene naphthalates (PEN) FRP [30, 31]. These types of unidirectional FRP composites are referred to as conventional FRPs in this paper. There are several benefits of using FRP(s) as a strengthening material, i.e. high strength to weight ratio and exceptional resistance to corrosion. The polymer is usually an epoxy and vinyl ester and phenol-formaldehyde resins are used. Among fibers, carbon fiber is the most expensive, and glass fiber is considered as the least expensive. Similarly, for polymers, epoxy polymer is considered as the most expensive as compared with vinyl ester and phenol-formaldehyde. Seible *et al.* [2] investigated the efficiency of continuous unidirectional carbon fiber reinforced polymer (CFRP) jacketing to increase the seismic performance of substandard bridge columns. The CFRP wrapping was applied to the circular or rectangular concrete columns with a variable jacket thickness along with the column height. The authors concluded that CFRP jacketing systems were very effective to improve the seismic response of substandard reinforced concrete columns. E-glass fiber – a more cost-effective alternative of CFRP – is also a composite wrapping material that has been experimentally investigated for the retrofitting and repairing of columns [1]. Dai *et al.* [31] carried out an experimental program to examine the seismic performance of reinforced concrete (RC) square columns retrofitted with polyethylene terephthalate (PET) FRP composites. It was concluded that PET FRP significantly enhances the displacement ductility of RC columns and hence can be taken into consideration as an alternative of conventional FRPs. In contrast to the unidirectional FRPs, recently a new method, i.e. sprayed glass fiber reinforced polymer composites, has been studied by many researchers [32–36]. The sprayed FRPs are also found very effective to enhance the strength and ductility of the strengthened structures. However, there are a few drawbacks in this method such as sprayed FRPs requiring special equipment, which is very expensive. Also, sprayed FRP required skilled labor because the thickness of sprayed FRP is difficult to control during the spraying process.

2. The significance of research

Although the conventional unidirectional FRPs are very successful in strengthening or retrofitting concrete structures, the cost of conventional FRPs is still considered to be prohibitive for the massive retrofit program of the existing buildings, especially for the developing countries. Hence, there is a need to develop more economical and affordable jacketing systems to enhance the strength and ductility of substandard structures. Currently, in Thailand, the boating industry is frequently utilizing very low-cost bi-directional glass fiber reinforced polymer composite (LC-GFRP) to manufacture the boats. The price of the bi-directional glass fiber sheet is only USD 2 per square

meter. Whereas the unit price of unidirectional carbon fiber reinforced polymer composite is USD 60 per square meter. A detailed review of the existing literature revealed that so far LC-GFRP has not been used to strengthen reinforced concrete structures. This study is planned to investigate the strengthening efficiency of the LC-GFRP composite to strengthen RC structures. The salient features of the LC-GFRP composites are low cost, wide availability and being more environmentally friendly. Also, the proposed LC-GFRP composites are bi-directional, thus these LC-GFRPs could protect the concrete against crushing and cracking much more effectively than the traditional unidirectional FRPs. Since LC-GFRP composites are low-cost, their application in real structures will be much more economical than carbon FRP composites. Further, a detailed survey of the existing bridge piers in Thailand indicates that most of them were constructed before the development of the current seismic codes in Thailand. Due to lateral reinforcement, the confinement in the existing bridge piers is insufficient. For example, in accordance with the code, the minimum required spacing for lateral reinforcement is $H/2$ (where H is section sectional height). However, it was found that in most of the bridge piers the provided minimum spacing is equal to H or even higher than H . A detailed review of the existing literature indicates that now there is little research on the seismic strengthening of the bridge piers. In the existing research, CFRP composite has been employed in different configurations to strengthen the bridge piers. However, there is no research on the seismic strengthening of the bridge piers by using GFRP composite. Therefore, it was planned to investigate the strengthening efficiency of the LC-GFRP composite to confine the insufficiently detailed bridge piers. To achieve the desired objective, an extensive experimental program was conducted. Three full-scale bridge piers were tested under lateral cyclic loading. One bridge pier was tested in the as-built condition, whereas the remaining two bridges piers were strengthened using an LC-GFRP jacketing system and tested under lateral loading.

3. An experimental program

To investigate the expected performance of bridge piers from LC-GFRP jacketing, three full-scale reinforced concrete bridge piers were constructed in this experimental study. The first bridge pier was tested in the as-built condition under lateral loading, i.e. without LC-GFRP jacketing. In this paper, the as-built bridge pier is referred to as P-01. The remaining two bridge piers, i.e. P-02 and P-03, were strengthened using low-cost bi-directional glass fiber sheets and tested under lateral loading. The strengthening of the bridge piers P-02 and P-03 was performed using two different strengthening configurations (Section 3.4).

3.1. Test specimen details. The details of the tested bridge piers also represent typical details of the existing construction practice of bridge piers in Thailand (Fig. 1). The details of the bridge piers are shown in Figs. 2a and 2b. The bridge piers are divided into two levels (Fig. 2a), i.e. lower level and upper level. The

lower level consists of the foundation, columns, and middle beam. The top-level consists of the top columns and top beam as shown in Fig. 2a. The full length at the foundation and height of bridge piers were 5000 mm and 3240 mm, respectively. The foundation had a cross-section of 500 (width)×350 (depth) mm. Each column (at the lower and upper level) had a cross-section of 200 (width)×2000 (depth) mm. The middle beam was constructed with a cross-section of 200 (width)×200 (depth) mm. The top beam had a cross-section of 250 (width)×300 (depth) mm. Each column contained 4 longitudinal deformed bars of No. 12 (4DB12). The transverse reinforcement in columns consisted of round bars of No. 6 provided at 200 mm spacing (RB6@200) throughout the column height. A lap splice of longitudinal reinforcement with a lap length of 400 mm was provided in the columns at lower levels. The middle beam contained 3 No. 12 deformed bars (3DB12) at each face, i.e. at the bottom and top faces. Similarly, the top beam consisted of 6 No. 12 deformed bars (6DB12) at each face, i.e. at the bottom and top faces. The bottom foundation was cast with 8 No. 12 deformed bars (8DB12) at each face, i.e. at the bottom and top faces. The web reinforcement in the top and middle beam consisted of round bars of No.6 placed at 120 mm (RB6@120) and 200 mm (RB6@200), respectively. The web reinforcement in the foundation consisted of round bars of No. 6 placed at 120 mm (RB6@120). The beam-column joints were constructed with extra reinforcement of 2 No. 12 deformed bars as shown in Fig. 2b. A clear 25 mm thick concrete cover was provided on all sides of beams, columns, and foundation.

3.2. Material properties. Ordinary Portland Cement (OPC) Type I and 19 mm downgraded coarse aggregates were used for preparing the concrete mixtures. Two types of mix designs were used to cast the bridge piers. The foundation was cast using high strength concrete, with 28-day target compressive strength of 50 MPa, to avoid any premature failure of the foundation. The columns and beams were cast using concrete with 28-day target compressive strength of 20 MPa. For each concrete mixture, three cylinders (150 mm in diameter and 300 mm in height) were cast in molds as per standard practice ASTM C31/C31M-12 [37]. The compressive strength test on these cylindrical specimens was conducted according to ASTM Standard ASTM C39/C39M [38]. The actual concrete strengths obtained during the testing days (around 35–45 days after casting) were slightly higher than the target design strengths, as shown in Table 1. Steel bars were tested in Universal Testing

Table 1
 Concrete compressive strength results (at test age)

Cylinder specimen	Lower column (MPa)	Middle beam (MPa)	Top column (MPa)	Top beam (MPa)
C-01	22.1	26.0	24.7	22.7
C-02	22.3	22.0	24.3	25.0
C-03	22.0	22.4	16.0	21.2
Average	22.1	23.5	21.6	22.9



Fig. 1. An existing bridge pier constructed in Thailand

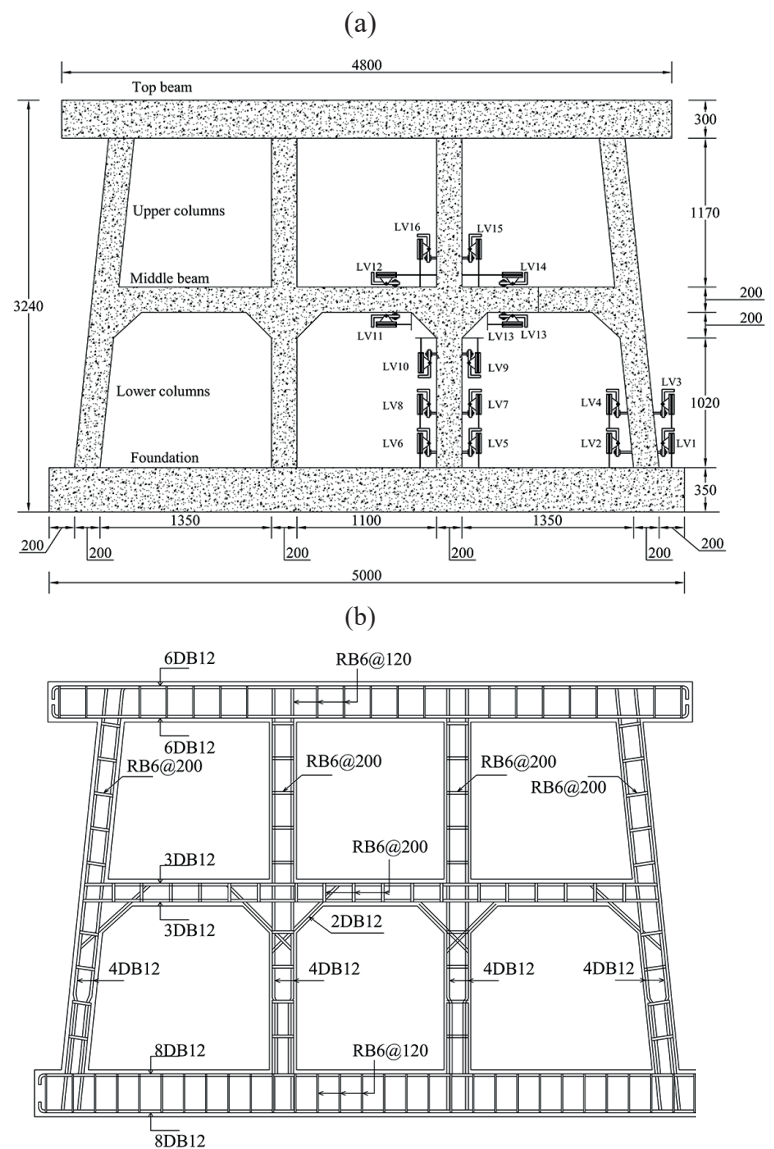


Fig. 2. a) Details of tested bridge pier, b) Reinforcement details (units in mm)

Table 2
Tensile properties of reinforced steel

Reinforced steel	Specimen	Yield strength f_y (MPa)	Modulus of elasticity E_s (MPa)	Yielding strain ϵ_y ($\mu\text{m/m}$)
Round steel bars \varnothing 6 mm	1	420.9	1.26.E+05	335.1
	2	426.1	1.26.E+05	339.4
	3	430.9	1.26.E+05	343.2
	Average	426.0	1.26.E+05	339.2
Deformed steel bars \varnothing 12 mm	1	573.2	1.98.E+05	289.8
	2	548.2	1.70.E+05	322.2
	3	523.4	1.76.E+05	297.6
	Average	548.3	1.81.E+05	303.2

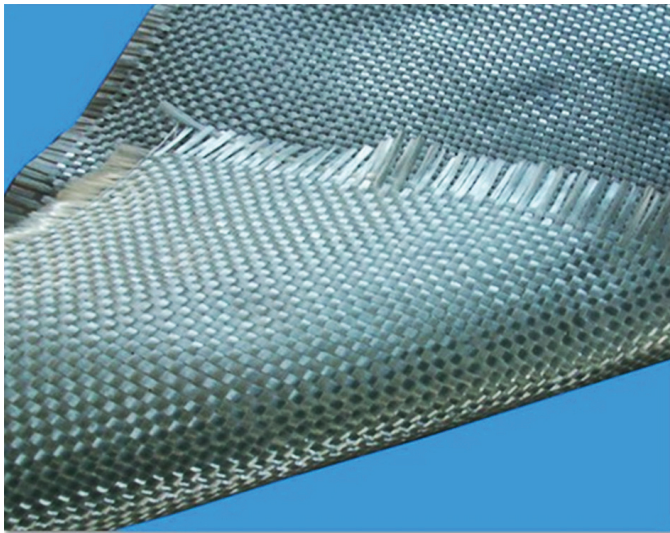


Fig. 3. Glass fiber sheet

Machine (UTM), as per ASTM standard ASTM E8 [39], to obtain the yield strength and ultimate strength of steel bars. Three samples were prepared for each size of steel bars and the average value was taken as the representative yield strength, modulus of elasticity, and yielding strain. The test results are summarized in Table 2. The strengthening of the bridge piers was performed using bi-directional E177 glass fiber sheets of 0.5 mm thickness (Fig. 3). The epoxy system used in the current research work consisted of resin and hardener, mixed in the ratio 3:1. Thorough and vigorous mixing of the resin and the hardener was carried out for at least 5 minutes using a mixing tool to ensure a consistent and homogenous product. The mechanical properties of LC-GFRP composite including the tensile strength and the modulus of elasticity were determined through tensile testing of flat coupons. The typical details of a flat coupon are shown in Fig. 4. The tensile test was performed on three tensile coupons following ASTM specification D3039-75 [40] and the resulting average values of the mechanical properties are summarized in Table 3. The typical failure of the GFRP strip is shown in Fig. 5a. Moreover, the tensile strength and the modulus of elasticity were obtained using the area of fiber rather than the gross cross-sectional area of the coupons. The stress-strain behavior of the LC-GFRP tensile coupon is shown in Fig. 5b.

Table 3
Mechanical properties of LC-GFRP

Specimen	Maximum tensile strength f_u (MPa)	Modulus of elasticity E (MPa)	Ultimate strain ϵ_u (%)
1	212.7	14655.0	1.57
2	207.3	14059.0	1.85
3	194.9	13943.0	1.77
Average	204.9	14219.0	1.73

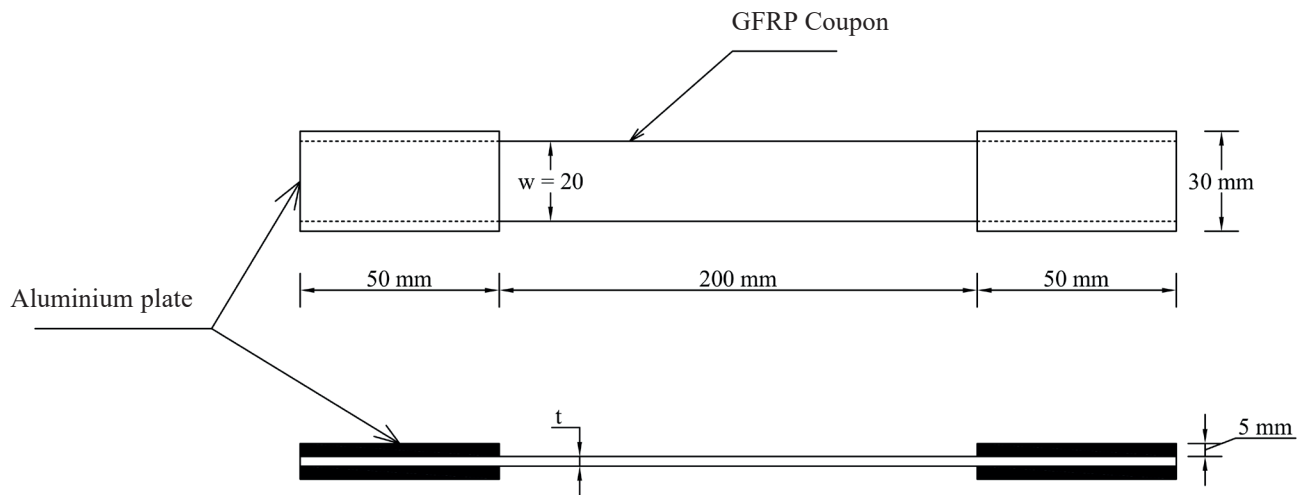


Fig. 4. LC-GFRP tension coupon details (units in mm)

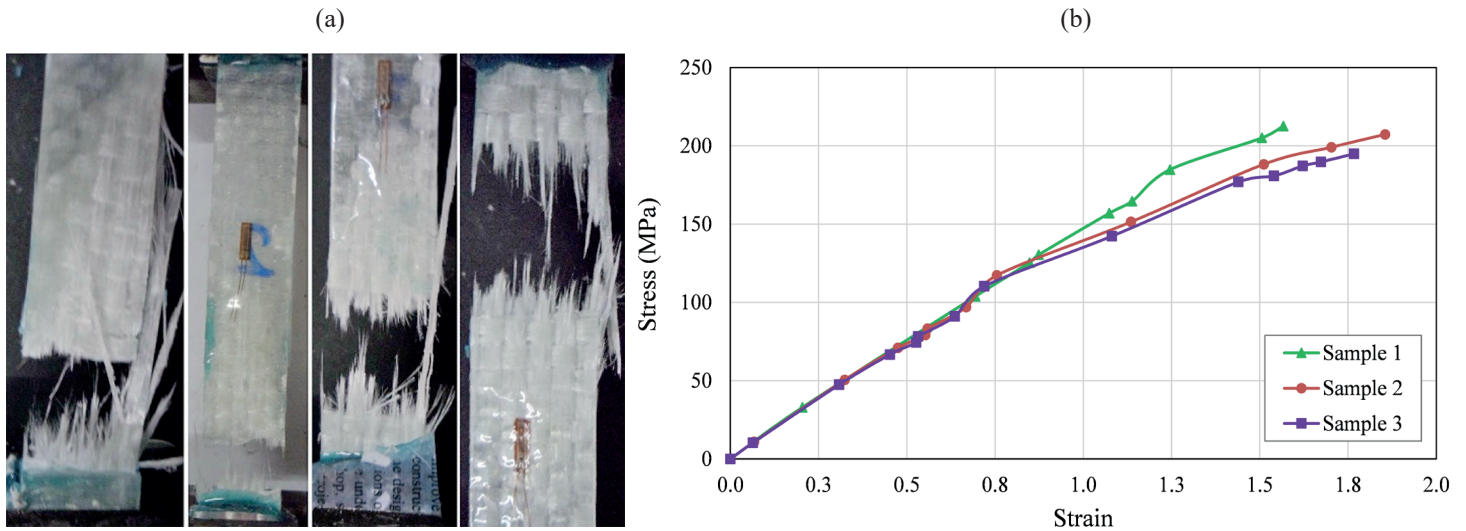


Fig. 5. a) Failure of GFRP strips [41], b) Stress versus strain behavior of GFRP composite

3.3. GFRP strengthening. In this study, LC-GFRP was applied in two different configurations, namely configuration A and configuration B. In configuration A, the lower level columns were fully wrapped, the upper-level columns were partially strengthened (i.e. fiber was only applied in the upper and lower regions of the columns), and the middle beams were fully wrapped as shown in Fig. 6a. The unstrengthened zones in configuration A were mainly beam-column joints and middle portion of the upper-level columns as shown in Fig. 6a. The strengthening configuration B was like the strengthening configuration A, except for the fact that the beam-column joints were also strengthened using bi-directional glass fiber sheets as shown in Fig. 6b. In previous work of the same research group [41], the authors performed different laboratory tests on axial compression of the concrete confined with the proposed strengthening method using different layers, i.e. 1, 2, and 3 layers. The results indicated the highest increase in the load-carrying capacity with three layers of GFRP. How-

ever, in the current study, four layers of bi-directional glass fiber sheets were applied for both strengthening configurations. The LC-GFRP jacket system includes the application of bi-directional glass fiber sheets on epoxy saturated surfaces. The surface of the concrete members to be strengthened with LC-GFRP was grinded before the application of LC-GFRP. A thin layer of epoxy was applied to the concrete surface and the GFRP sheet was then attached to the surface of epoxy. For each layer of glass fiber sheet, two plies of epoxy, one on the concrete surface right before installing the sheet and the other on the surface of the installed sheet, were applied using paintbrush or rollers to ensure fully saturated glass fiber layers with epoxy. During the installation of the fiber sheets, extreme care was taken to avoid any gaps between the fiber sheets and the concrete surface. After the required layers of the sheet were installed, the LC-GFRP composite jacket was cured in the ambient condition. The installation of LC-GFRP sheets is shown in Fig. 7.

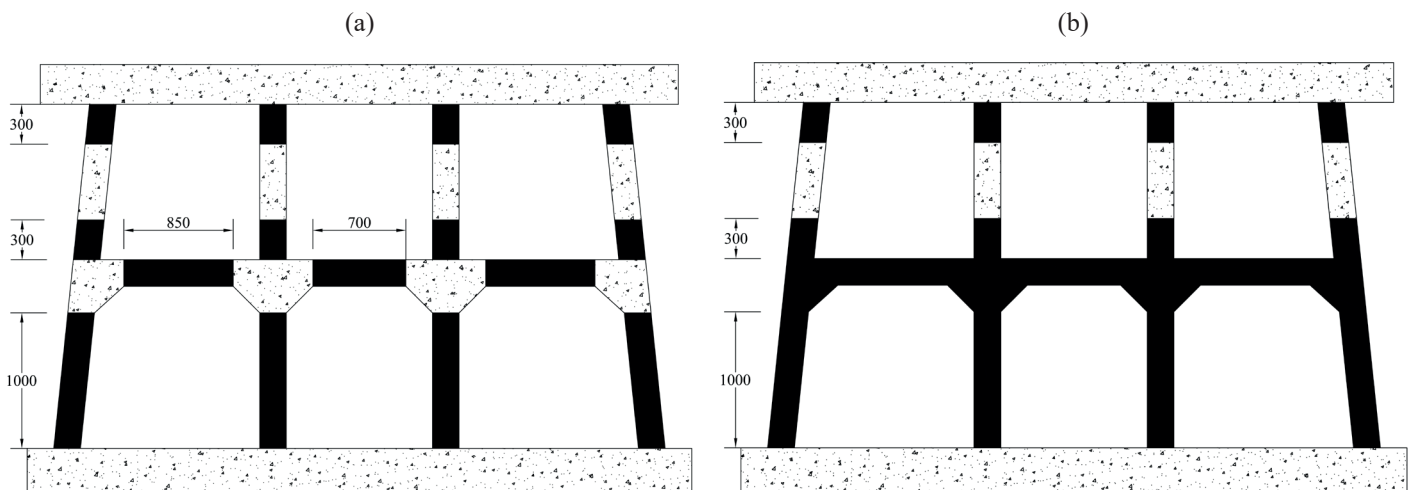


Fig. 6. Strengthening configuration: a) A, b) B



Fig. 7. Installation of the glass fiber sheet

3.4. Instrumentation and load setup. As concrete structures are frequently exposed to cyclic loading during the service life [42], in this study the tested bridge piers were subjected to reverse cyclic tests in the laboratory of the King Mongkut University of Thailand. A total of 16 LVDTs were installed at different locations of the bridge piers to record the required necessary data at different deformation steps as shown in Fig. 2a. In addition to the LVDTs, strain gauges (gauge length = 5 mm) were also installed on longitudinal and lateral steel bars to deter-

mine strain values during the test. The bridge pier foundation was anchored to the strong floor with steel rods and bolts to avoid the overturning movements. The lateral load was applied using a horizontally installed hydraulic actuator to simulate the seismic demand. The loading set up is shown in Fig. 8a. The out-of-plane movement was prevented by using lateral supports as shown in Fig. 8b. The quasi-static lateral cyclic loading history was employed to apply the cyclic loading as proposed by Priestley and Park [43]. The displacement control loading scheme consisted of two consecutive cycles at each drift level as shown in Fig. 9. The bridge piers were subjected to reversed cyclic loads using a target percent drift of ± 0.25 , ± 0.5 , ± 0.75 , ± 1.0 , ± 1.5 , ± 2.0 , ± 2.5 , ± 3.0 , and so on. The drift ratio is defined as the lateral displacement normalized by the height measured from the top of the bottom plate to the point of lateral load application. The hydraulic actuator was manually operated in a displacement control mode.

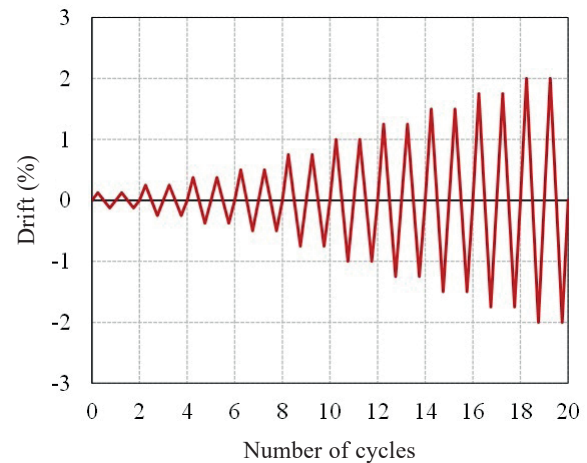


Fig. 9. Loading history

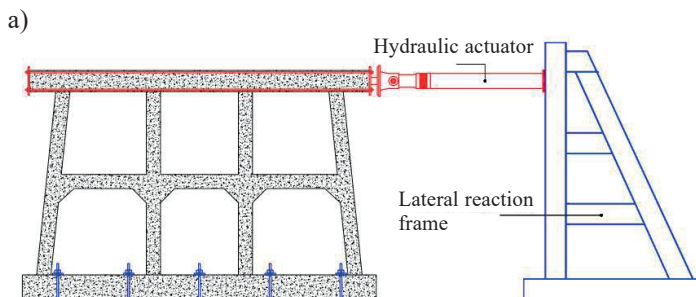


Fig. 8. a) Loading setup (units in mm), b) Lateral supports to prevent out-of-plane movement of bridge piers

4. Test results and discussions

In this study, three full-scale bridge piers were tested under lateral cyclic loading. The tests were performed using the same loading setup. The experimental results are discussed in the following sections.

4.1. Failure modes.

4.1.1. As-built bridge pier (P-01). The bridge pier P-01 (as-built bridge pier) remained undamaged until the drift level of 0.25%. The first visible flexure cracks were observed at the drift level of 0.50% on columns and beams, as shown in Fig. 10a. A few inclined cracks were also observed on the interior beam-column joints. However, the exterior beam-column joints were undamaged at this stage. The number of flexural cracks increased when the lateral drift ratio was increased. At 0.75% and 1.00% drift level, flexural cracks appeared at the location of exterior beam-column joints (Figs. 10b and 10c). The increase in lateral drift resulted in the increased flexural cracking. During the first cycle of 1.5% drift ratio, the peak lateral strength was achieved,



Fig. 10. Damage to the bridge pier P-01 at the lateral drift of: a) 0.50%, b) 0.75%, c) 1.00%, d) 1.50%

and at the same time, the concrete cover began to spall in the lower level columns and middle beam. The onset of a major shear crack in the plastic hinge zone of lower columns and middle beams and a corresponding drop in the lateral strength were observed during the second cycle of 1.5% drift ratio (Fig. 10d). At this stage, the test was terminated to avoid any damage to the instruments and other lab facilities. The line diagram of cracking in the specimen P-01 is shown in Fig. 11.

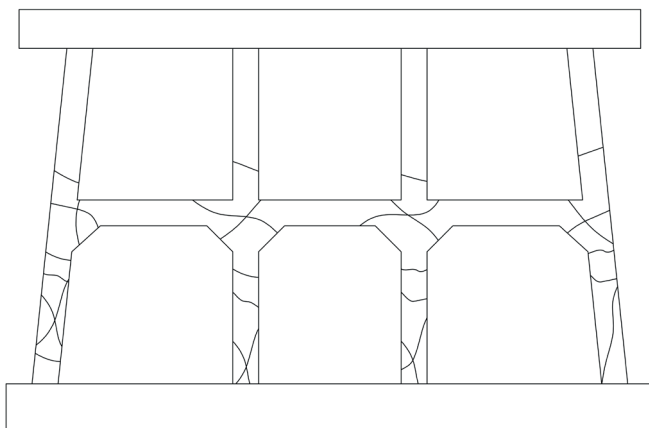


Fig. 11. Line diagram of cracking in the bridge pier P-01

4.1.2. LC-GFRP Strengthened Bridge Pier (P-02). The LC-GFRP strengthened bridge pier, i.e. P-02 (strengthened using configuration A) showed much improvement in behavior in terms of lateral load-carrying capacity and ductility, as compared to the unstrengthened bridge pier (i.e. P-01). The LC-GFRP strengthened bridge pier (i.e. P-02) was also undamaged up to the drift level of 0.25%. Unlike on the bridge pier P-01, initial flexural cracks were observed at the drift level of 0.50% at the location of interior and exterior beam-column joints. The results suggest that GFRP strengthening of beams and columns can shift failure from beams and columns towards the joint zone. The increase in the lateral drift resulted in increased flexural cracking. With further increase in the lateral drift level, i.e. at drift level of 0.75%, the initially observed cracks grew, both in terms of width and length. At this stage, new cracks were also observed at the location of the interior and exterior beam-column joints. A slight crushing of the concrete at the base of the upper-level columns was observed at the drift level of 1.00% (Fig. 12a). Severe damage and numerous cracks were observed on the interior and exterior beam-column joints, at the drift level of 2.00% (Fig. 12b). With further growth of the drift level, i.e. 3.00% and 3.50%, significant crushing and spalling of concrete were experienced on the interior and exterior beam-column joints, as shown in Figs. 12c and d. However, the unstrengthened portion of the



Fig. 12. Damage to the bridge pier P-02 at the lateral drift of: a) 0.50%, b) 0.75%, c) 1.00%, d) 1.50%

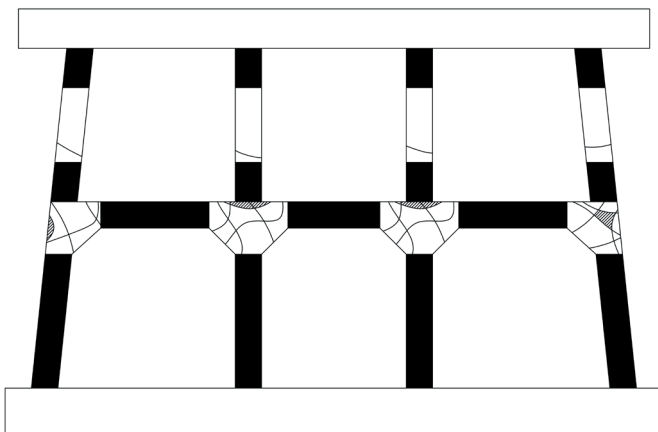


Fig. 13. Line diagram of cracking in the bridge pier P-02

upper-level columns remained undamaged throughout the test. The line diagram of cracking in the specimen P-02 is presented here in Fig. 13.

4.1.3. LC-GFRP Strengthened Bridge Pier (P-03). Similar to the bridge pier P-02, the LC-GFRP strengthened bridge pier, i.e. P-03 (strengthened using configuration B) also showed sig-

nificantly improved behavior in terms of the lateral load-carrying capacity and ductility, as compared to the unstrengthened bridge pier (i.e. P-01). The bridge pier P-03 remained undamaged until the drift level of 0.25%. In contrast to the bridge pier P-02, the first visible cracks were observed at the drift level of 0.50% in the unstrengthened zone of the upper-level columns, indicating that the strengthening of beam-column joints can shift the failure from the joint core towards the weak columns (Fig. 14a). This further indicated the effectiveness of LC-GFRP confinement to the beams, columns, and beam-column joints. The increase in the lateral drift resulted in the increased flexural cracking. At 1.25% drift ratio, the peak lateral strength was attained, and at the same time, the concrete cover began to spall (Fig. 14b). At 2.0% drift ratio, a major shear crack was observed along with a corresponding drop in the lateral strength (Fig. 14c). At the same drift level, inclined cracks were also observed on the top beam. At 4.0% drift ratio (final drift ratio), the longitudinal reinforcement buckled due to the complete loss of concrete cover, as shown in Fig. 14d. The final failure of the LC-GFRP strengthened bridge pier (i.e. P-03) can be characterized as the shear failure of the upper-level columns in the unstrengthened middle zones, along with a slight damage to the top beam. The line diagram of cracking in the specimen P-03 is shown here as Fig. 15.



Fig. 14. Damage to the bridge pier P-03 at drift level of: a) 0.50%, b) 1.25%, c) 2.00%, d) 4.00%

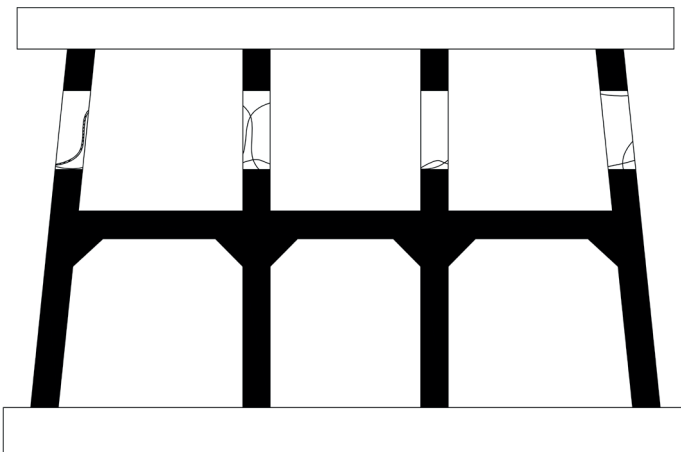


Fig. 15. Line diagram of cracking in the bridge pier P-03

4.2. Lateral load versus drift ratio responses. Experimental results in terms of the lateral load (P_y), displacement at the first yield (δ_y), the maximum load (P_{max}), the ultimate displacement (δ_u) and the displacement ductility factor (μ_ϵ) are summarized in Tables 4 and 5. The ultimate displacement (δ_u)

Table 4
Experimental test results in terms of lateral load

Specimen	Yielding lateral load P_y (kN)	% Increase in yielding lateral load	Maximum load P_{max} (kN)	% Increase in maximum load
P-01	45.70	–	96.30	–
P-02	78.40	42.0	104.50	8.0
P-03	101.63	55.0	111.70	14.0

Table 5
Experimental test results in terms of drift and ductility

Specimen	Yielding drift δ_y	% Increase in yielding drift	Ultimate drift* δ_u	% Increase in ultimate drift	Ductility factor $\mu_\epsilon = \delta_u/\delta_y$
P-01	0.50	–	1.50	–	3.00
P-02	0.75	33.0	3.50	57.0	4.67
P-03	1.00	50.0	3.50	57.0	3.50

* Displacement at which a drop of the load from P_{max} to $P_{80\%}$ was observed [44, 45]

was defined as that at which a drop of the load from P_{max} to $P_{80\%}$ was observed [44, 45] and the ductility factor was considered as the ratio between the ultimate displacement and first yield displacement (δ_u and δ_y). The experimental responses of as-built and LC-GFRP strengthened bridge piers are shown in Figs. 16 a-f in the form of lateral load versus drift ratio. The

envelope curves of the unstrengthened and strengthened bridge piers are shown in Fig. 17.

The reference bridge pier specimen (P-01) failed in a brittle manner by a rapid widening of diagonal cracks in the plastic hinge zone of the lower columns and beam-column joints, leading to a sudden drop of the load-carrying capacity from

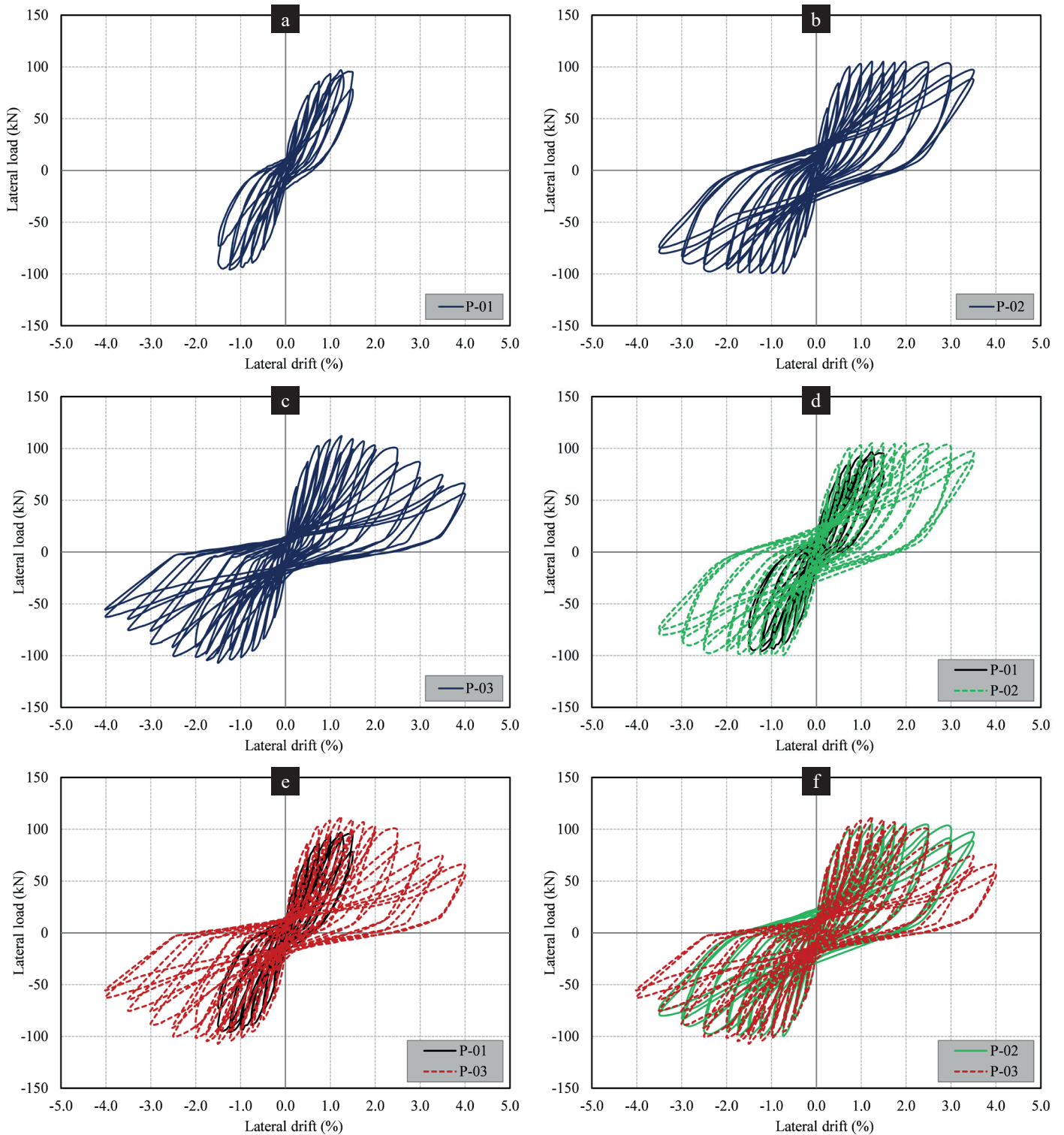


Fig. 16. Lateral load versus drift ratio response of bridge pier: a) P-01, b) P-02, c) P-03, d) P-01 and P-02, e) P-01 and P-03, f) P-02 and P-03

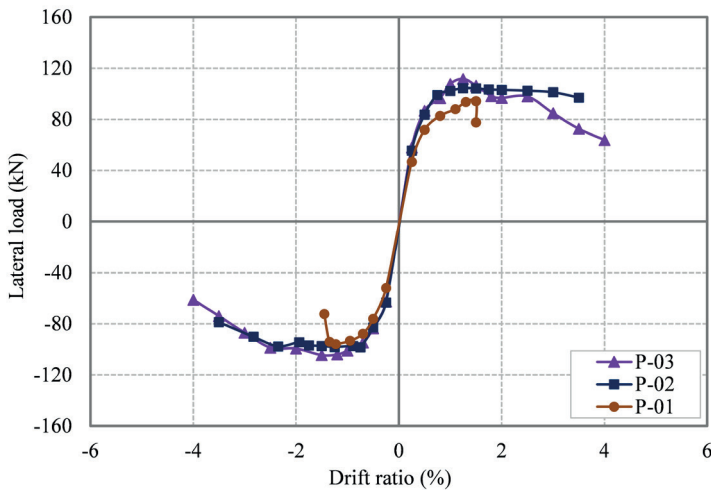


Fig. 17. Envelop or skeleton curves of tested bridge piers P-01, P-02, and P-03

the peak when the load was applied during the second cycle of 1.50% drift ratio. The bridge pier P-01 achieved its maximum lateral load capacity of 96.30 kN at 1.50% drift ratio. Severe cracking and spalling of concrete cover were observed during the second cycle of 1.50% drift ratio (Fig. 10d). The test was then terminated to avoid damage to the instruments and lab facilities. The pier specimen (P-02) mainly failed due to the significant crushing and spalling of concrete on the interior and exterior beam-column joints. Comparing the bridge piers P-01 and P-02 (Fig. 16d), the behavior of the bridge pier P-02 was more ductile, with a ductility factor μ_ϵ of 4.67. The bridge pier P-02 achieved its maximum lateral load capacity of 104.50 kN at 1.25% drift level. The maximum lateral load, ultimate displacement, and ductility ratio were found to be 8%, 57%, and 36% higher, respectively, as compared to the unstrengthened bridge pier P-01. It was noted that the descending branch after the peak strength at 3.50% drift ratio was very smooth since there were no serious damages found, indicating the effectiveness of LC-GFRP confinement.

Similar to the bridge pier P-02, the behavior of bridge pier P-03 was more ductile as compared to the as-built bridge pier (P-01), with a ductility factor μ_ϵ of 3.50. By comparing specimen P-01 and P-03, it can be noted that the drift capacity of P-03 was greatly enhanced due to the confinement effect. The bridge pier P-03 achieved its maximum lateral load capacity of 111.70 kN at 1.25% drift level. The maximum lateral load, ultimate displacement, and ductility ratio were found to be 14%, 57%, and 14% higher, respectively, as compared to the unstrengthened bridge pier P-01. By comparing specimens P-02 and P-03 (Fig. 16 f), it can be observed that the lateral load-carrying capacity of P-03 was higher than that of the bridge pier P-02. However, the ductility of the bridge pier P-03 was found lower than that of the bridge pier P-02. This was supposedly due to the higher level of confinement of the lower zone of the bridge pier (i.e. lower-level columns, middle beam, and beam-column joints), thus making the upper-level columns very weak in the middle of the not strengthened zone.

It can also be noticed that at 1.25% drift ratio, the descending branch after the peak strength dropped sharply as compared to the bridge pier P-02, indicating serious damage to the bridge pier. This was supposedly due to the shear failure of the columns at the upper level. In this bridge pier, i.e. P-03, at 3.00% drift ratio until the end of the test, severe crushing and spalling of concrete was observed in the middle zone of the upper-level columns. The buckling of longitudinal steel bars was also seen in the not strengthened zones of the upper-level columns. It is evident from the experimental results that the proposed strengthening method is very useful to alter the seismic performance of the nonductile bridge piers in terms of ultimate load-carrying capacity, ultimate displacement, and ductility. In this study, the maximum increase in the lateral load-carrying capacity was found to be 16% for the bridge pier 02. A study conducted on the flexural strengthening of the bridge piers using three layers of traditional carbon fiber reinforced polymer composites reported a maximum increase of 8.0% as compared to the unstrengthened bridge pier [46]. In another study, 10 layers of traditional carbon fiber reinforced polymer composites were used to strengthen the bridge pier. Experimental results indicated a maximum of 17.0% increase in the lateral load-carrying capacity of the CFRP strengthened specimen [47]. This is a very clear indication that the proposed strengthening method is very effective and could be replaced with the existing methods.

4.3. Stiffness of bridge piers. The effectiveness of LC-GFRP strengthening techniques used to enhance the stiffness of bridge piers was assessed by plotting the stiffness curves (instantaneous secant stiffness at a certain displacement) of LC-GFRP strengthened bridge piers along with the unstrengthened bridge pier, i.e. P-01 in Fig. 18. It can be observed in Fig. 18 that a positive value of the cycle number corresponds to a loading cycle involving upward lateral displacement and negative values are related to the cycles involving downward displacement. It can

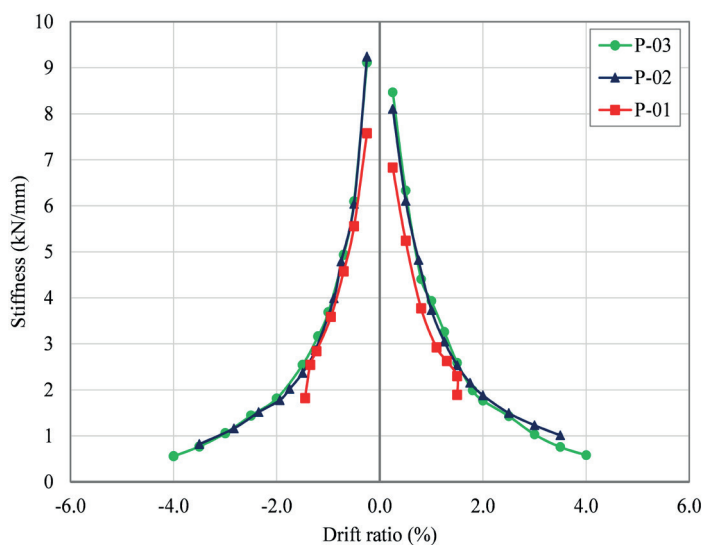


Fig. 18. Stiffness of tested bridge piers

be seen that the LC-GFRP strengthening technique was found to be very effective in increasing the overall stiffness of LC380 GFRP strengthened bridge piers. However, the initial stiffness of both LC-GFRP strengthened bridge piers exhibited an almost similar trend, as shown in Fig. 18.

4.4. Cumulative dissipated energy of LC-GFRP strengthened bridge piers. The cumulative hysteretic dissipation energy was evaluated for all tests, considering the area of each loading cycle in the X and Y direction, and then the total energy was calculated as the sum of these two parts. The cumulative energy dissipated was then obtained by summing the energy dissipated in consecutive cycles throughout the test. The cumulative energy dissipation versus the lateral drift ratio is presented in Fig. 19 and it can be seen that LC-GFRP strengthened RC columns permit to dissipate more energy compared with the un-strengthened specimen. This was mainly due to the additional confinement provided by the LC-GFRP jackets.

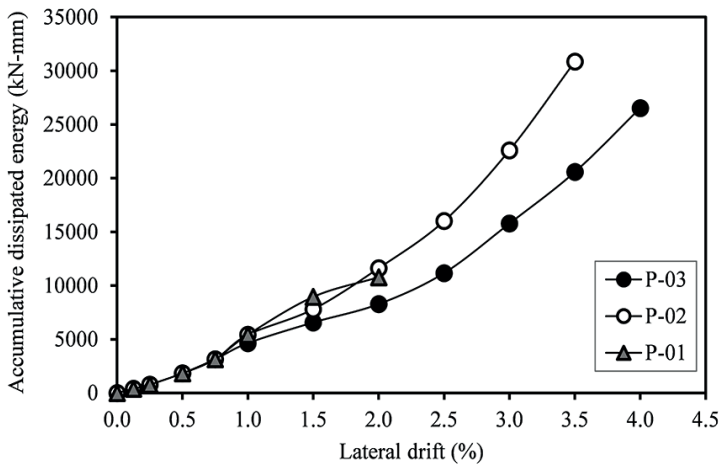


Fig. 19. Accumulative dissipated energy versus lateral drift ratio for different cases considered

4.5. Ductility of the LC-GFRP strengthened bridge piers. The displacement ductility ratio μ_ϵ is defined as the ratio between ultimate displacement and yielding displacement. The bridge piers with a larger ductility ratio had better ductility properties. The displacement ductility ratio of the tested bridge piers is summarized in Table 4. A comparison of skeleton curves of the LC-GFRP strengthened and unstrengthened bridge pier is also shown in Fig. 17. The experimental test results showed that the LC-GFRP strengthening technique is very effective to alter and enhance the ductility of strengthened bridge piers. The ductility of the LC-GFRP strengthened bridge piers P-02 and P-03 was recorded as 56% and 17% higher, respectively, as compared to the unstrengthened bridge pier, i.e. P-01. The ductility of the LC402 GFRP strengthened bridge pier P-03 was recorded lower than the ductility of the bridge pier P-02. This phenomenon is associated with the shear failure of the upper-level columns in the case of the LC404 GFRP strengthened bridge pier P-03, as shown in Fig. 14d.

4.6. Effect of the LC-GFRP strengthening configuration. In this experimental study, two types of strengthening configurations, i.e. Type A and Type B (Figs. 6a and 6b), were adopted to study the structural response of the LC-GFRP strengthened bridge piers. To investigate the effect of strengthening configurations, a comparison of lateral load versus lateral drift of the unstrengthened and LC-GFRP strengthened bridge pier is shown in Figs. 16 d-f. Accumulated energy dissipation of the bridge piers P-01, P-02, and P-03 is shown in Fig. 17. A graphical comparison showing the load and displacement of both unstrengthened and LC-GFRP strengthened bridge piers is also displayed in Figs. 20 and 21. It can be seen that the bridge pier (P-02), which was strengthened using strengthening configuration B, showed superior behavior over the bridge pier P-01. As compared to the unstrengthened bridge pier (P-01), the increase in the lateral yielding load was 71% and 122% for the strengthening configurations A and B, respectively. Moreover, the maximum lateral load was increased by 8% and 16% for the strengthening configurations A and B, respectively, as compared to the un-strengthened bridge pier (P-01). Similarly, the yielding displacement was increased by 50% and 100% for the bridge piers P-02 and P-03, respectively, as compared

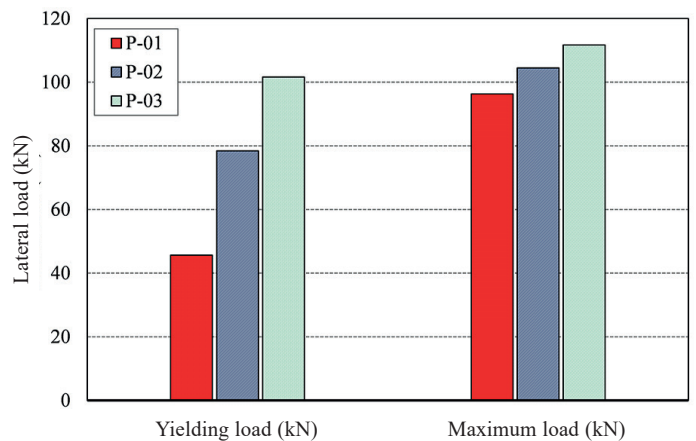
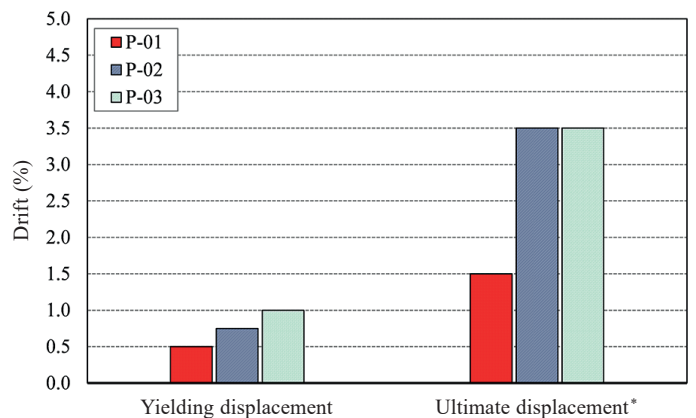


Fig. 20. The effect of strengthening configuration on lateral load carrying capacity of bridge piers



* Displacement at which a drop of the load from P_{max} to 80% was observed

Fig. 21. The effect of strengthening configuration on displacement

to the bridge pier P-01. Ultimate displacement was increased by 133% for both the bridge piers P-02 and P-03, as compared to the bridge pier P-01. The strengthening configuration B also dissipated higher accumulative energy as compared to the strengthening configuration A (Fig. 19). Better performance of the strengthening configuration B was due to the confinement of the beam-column joint, as compared to the strengthening configuration A.

5. Conclusions

This paper presents the experimental study of strengthening non-ductile reinforced concrete bridge piers by low cast glass fiber reinforced polymers (LC-GFRP) jacketing under quasi-static cyclic lateral loading. Three full-scale bridge piers were tested under lateral cyclic loading. A control bridge pier was tested under the as-built condition and the other two bridge piers were experimentally tested after being strengthened with LC-GFRP jacketing. Based on the experimental outcome, the following conclusions can be drawn:

1. The control or as-built bridge pier showed a poor seismic response with the development of significant cracks at very low drift levels.
2. LC-GFRP strengthening has proved to every effective in altering the seismic response of full-scale RC bridge piers.
3. The test results suggest that LC-GFRP strengthening of the beams, columns and beam-column joints in bridge piers can shift failure from a brittle mode to a ductile mode.
4. The final failure of the bridge pier strengthened using configuration A (unstrengthened beam-column joints) was mainly due to the failure of beam-column joints.
5. The bridge pier strengthened using configuration B (strengthened beam-column joints) failed mainly due to the shear failure of the columns at the upper level.
6. In terms of lateral load-carrying capacity, the strengthening configuration B is found superior to the strengthening configuration A.

Acknowledgment. The authors are grateful to the National Research Council of Thailand (contract no. KMUTNB-GOV-60-009) for providing a full funding support to complete the research. Thanks are extended to the Department of Teacher Training in Civil Engineering, King Mongkut's University of Technology North Bangkok for providing the test facilities.

REFERENCES

- [1] M.J. Priestley, "Column retrofitting using fibreglass/epoxy jackets", in *1st Annual Seismic Research Workshop. CalTrans, Sacramento*, 1991, pp. 217–224.
- [2] F. Seible, M.J.N. Priestley, G. A. Hegemier, and D. Innamorato, "Seismic retrofit of RC columns with continuous carbon fiber jackets", *J. Compos. Constr.* 1(2), 52–62 (1997).
- [3] B.A. Bolt, W.L. Horn, G.A. MacDonald, and R.F. Scott, *Geological Hazards: Earthquakes-tsunamis-volcanoes-avalanches-landslides-floods*. Springer Science & Business Media, 2013.
- [4] A.S. Nowak, "System reliability models for bridge structures", *Bull. Pol. Ac.: Tech.* 52(4), 321–328 (2004).
- [5] B. Goszczyńska, G. Świt, and W. Trąpczyński, "Analysis of the microcracking process with the Acoustic Emission method with respect to the service life of reinforced concrete structures with the example of the RC beams", *Bull. Pol. Ac.: Tech.* 63(1), 55–63 (2015).
- [6] P. Tirasit and K. Kawashima, "Seismic performance of square reinforced concrete columns under combined cyclic flexural and torsional loadings", *J. Earthq. Eng.* 11(3), 425–452 (2007).
- [7] K.J. Fridley and Z. Ma, *Reliability-based design of seismic retrofit for bridges*. Department of Transportation, 2009.
- [8] A. Ghobarah, T.S. Aziz, and A. Biddah, "Rehabilitation of reinforced concrete frame connections using corrugated steel jacketing", *Struct. J.* 94(3), 282–294 (1997).
- [9] C. Suesuttajit, "A survey of configuration irregularities in typical multi-story concrete buildings in Thailand", Asian Institute of Technology, Thailand, 2007.
- [10] K. Rodsin, T. Mehmood, K. Kolozviri, and A. Nawaz, "Seismic assessment of non-engineered reinforced concrete columns in low to moderate seismic regions", *Bull. Earthq. Eng.* 18, 5941–5964 (2020).
- [11] K. Rodsin, P. Warnitchai, and T. Awan, "Ultimate drift at gravity load collapse of non-ductile RC columns", in *5th Civil Engineering Conference in the Asian Region and Australasian Structural Engineering Conference 2010*, Sydney, Australia, 2010, p. 441.
- [12] P. Juntanalikit, T. Jirawattanasomkul, and A. Pimanmas, "Experimental and numerical study of strengthening non-ductile RC columns with and without lap splice by Carbon fiber reinforced polymer (CFRP) jacketing", *Eng. Struct.* 125, 400–418 (2016).
- [13] A. Garbacz, L. Courard, and B. Bissonnette, "A surface engineering approach applicable to concrete repair engineering", *Bull. Pol. Ac.: Tech.* 61(1), 73–84 (2013V).
- [14] M. Suarjana, D.D. Octora, and M. Riyansyah, "Seismic Performance of RC Hollow Rectangular Bridge Piers Retrofitted by Concrete Jacketing Considering the Initial Load and Interface Slip", *J. Eng. Technol. Sci.* 52(3), 343–369 (2020).
- [15] A. Algburi, N. Sheikh, and M. Hadi, "Analysis of concrete columns with high-performance concrete jackets and polymer wraps", *Proc. Inst. Civ. Eng. Build.*, 1–33 (2020). doi: 10.1680/jstbu.19.00195.
- [16] P.S. Theint, A. Ruangrassamee, and Q. Hussain, "Strengthening of shear-critical RC columns by high-strength steel-rod collars", *Eng. J.* 24(3), 107–128 (2020).
- [17] D. Zhang, N. Li, Z.-X. Li, and L. Xie, "Experimental investigation and confinement model of composite confined concrete using steel jacket and prestressed steel hoop", *Constr. Build. Mater.* 256, 119399 (2020).
- [18] X. Zhao, H. Liang, Y. Lu, and P. Zhao, "Size effect of square steel tube and sandwiched concrete jacketed circular RC columns under axial compression", *J. Constr. Steel Res.* 166, 105912 (2020).
- [19] A. Gholampour, R. Hassanli, J.E. Mills, T. Vincent, and M. Kunnieda, "Experimental investigation of the performance of concrete columns strengthened with fiber reinforced concrete jacket", *Constr. Build. Mater.* 194, 51–61 (2019).
- [20] S.W.N. Razvi and M.G. Shaikh, "Effect of confinement on behavior of short concrete column", *Procedia Manuf.* 20, 563–570 (2018).
- [21] P. Nagaprasad, D.R. Sahoo, and D.C. Rai, "Seismic strengthening of RC columns using external steel cage", *Earthq. Eng. Struct. Dyn.* 38(14), 1563–1586 (2009).

- [22] S. Ochelski, P. Bogusz, and A. Kiczko, "Static axial crush performance of unfilled and foamed-filled composite tubes", *Bull. Pol. Ac.: Tech.* 60(1), 31–35 (2012).
- [23] L.C. Bank, *Composites for construction: Structural design with FRP materials*. John Wiley & Sons, 2006.
- [24] Q. Hussain, A. Ruangrassamee, S. Tangtermsirikul, and P. Joyklad, "Behavior of concrete confined with epoxy bonded fiber ropes under axial load", *Constr. Build. Mater.* 263, 120093 (2020).
- [25] Q. Hussain, "A study on sprayed fiber reinforced polymer composites for strengthening of reinforced concrete members", 2015.
- [26] Y. Xiao and R. Ma, "Seismic retrofit of RC circular columns using prefabricated composite jacketing", *J. Struct. Eng.* 123(10), 1357–1364 (1997).
- [27] H.F. Isleem, D. Wang, and Z. Wang, "Axial stress–strain model for square concrete columns internally confined with GFRP hoops", *Mag. Concr. Res.* 70(20), 1064–1079 (2018).
- [28] O.S. AlAjarmeh, A.C. Manalo, B. Benmokrane, W. Karunasena, and P. Mendis, "Effect of spiral spacing and concrete strength on behavior of GFRP-reinforced hollow concrete columns", *J. Compos. Constr.* 24(1), 4019054 (2020).
- [29] P. Rochette and P. Labossiere, "Axial testing of rectangular column models confined with composites", *J. Compos. Constr.* 4(3), 129–136 (2000).
- [30] J.-G. Dai, Y.-L. Bai, and J.G. Teng, "Behavior and modeling of concrete confined with FRP composites of large deformability", *J. Compos. Constr.* 15(6), 963–973 (2011).
- [31] J.-G. Dai, L. Lam, and T. Ueda, "Seismic retrofit of square RC columns with polyethylene terephthalate (PET) fibre reinforced polymer composites", *Constr. Build. Mater.* 27(1), 206–217 (2012).
- [32] Q. Hussain and A. Pimanmas, "Shear strengthening of RC deep beams with openings using sprayed glass fiber reinforced polymer composites (SGFRP): part 1. Experimental study", *KSCE J. Civ. Eng.* 19(7), 2121–2133 (2015).
- [33] Q. Hussain and A. Pimanmas, "Shear strengthening of RC deep beams with sprayed fiber-reinforced polymer composites (SFRP): Part 2 Finite element analysis", *Lat. Am. J. Solids Struct.* 12(7), 1266–1295 (2015).
- [34] Q. Hussain and A. Pimanmas, "Shear strengthening of RC deep beams with sprayed fibre-reinforced polymer composites (SFRP) and anchoring systems: Part 1. Experimental study", *Eur. J. Environ. Civ. Eng.* 20(1), 79–107 (2016).
- [35] Q. Hussain, W. Rattanapitikon, and A. Pimanmas, "Axial load behavior of circular and square concrete columns confined with sprayed fiber-reinforced polymer composites", *Polym. Compos.* 37(8), 2557–2567 (2016).
- [36] C.P. Pantelides, J. Gergely, L.D. Reaveley, and V.A. Volnyy, "Retrofit of RC bridge pier with CFRP advanced composites", *J. Struct. Eng.* 125(10), 1094–1099 (1999).
- [37] ASTM C31/C31M-12, *Standard practice for making and curing concrete test specimens in the field*. ASTM International, West Conshohocken, PA, USA, 2012.
- [38] ASTM C39/C39M, *Standard test method for compressive strength of cylindrical concrete specimens*. ASTM International, West Conshohocken, PA, USA, 2018.
- [39] ASTM E8, *Standard test methods for tension testing of metallic materials*. ASTM International, West Conshohocken, PA, USA, 2013.
- [40] ASTM Committee D-30 on Composite Materials, *Standard test method for tensile properties of polymer matrix composite materials*. ASTM International, West Conshohocken, PA, USA, 2008.
- [41] P. Yoddumrong, K. Rodsin, and S. Katawaethwarag, "Experimental study on compressive behavior of low and normal strength concrete confined by low-cost glass fiber reinforced polymers (GFRP)", in *2018 Third International Conference on Engineering Science and Innovative Technology (ESIT)*, 2018, pp. 1–4.
- [42] Y. Chen, X. Chen, and J. Bu, "Nonlinear damage accumulation of concrete subjected to variable amplitude fatigue loading", *Bull. Pol. Ac.: Tech.* 66(2), 157–163 (2018).
- [43] M.J.N. Priestley and R. Park, "Strength and ductility of concrete bridge columns under seismic loading", *Struct. J.* 84(1), 61–76 (1987).
- [44] M.J.N. Priestley, "Displacement-based seismic assessment of reinforced concrete buildings", *J. Earthq. Eng.* 1(1), 157–192 (1997).
- [45] M.N. Fardis, *Seismic design, assessment and retrofitting of concrete buildings: based on EN-Eurocode 8*. Springer Science & Business Media, 2009.
- [46] T. Alkhrdaji and A. Nanni, "Flexural strengthening of bridge piers using FRP composites", in *Advanced Technology in Structural Engineering*, 2000, pp. 1–13.
- [47] M.J.N. Priestley, F. Seible, and G.M. Calvi, *Seismic design and retrofit of bridges*. John Wiley & Sons, 1996.